nature

https://doi.org/10.1038/s41586-020-2412-8

Supplementary information

The first dinosaur egg was soft

In the format provided by the authors and unedited

Mark A. Norell✉, Jasmina Wiemann✉, Matteo Fabbri✉, Congyu Yu, Claudia A. Marsicano, Anita Moore-Nall, David J. Varricchio, Diego Pol & Darla K. Zelenitsky

Supplementary Note 1

The first dinosaur egg was soft

Mark Norell[1*], Jasmina Wiemann[2], Matteo Fabbri[2], Congyu Yu[1], Claudia A. Marsicano[3], Anita Moore-Nall[4], David Varricchio[4], Diego Pol[5], Darla K. Zelenitsky[6]

Supplementary Note 1 includes:

1. Selected eggshells and eggshell membranes

Supplementary Tab. 1: Specimen data.

Assigned Taxon	Catalogue No.	Age	Locality	Tissue
Phrynops hilarii	YPM HERR 18005	Quaternary	No locality data given	Eggshell membrane
Mesoclemmys gibba	YPM HERR 17990	Quaternary	No locality data given	Eggshell membrane
Emys orbicularis	To be catalogued	Quaternary	No locality data given	Eggshell membrane
Caiman yacare	To be catalogued	Quaternary	No locality data given	Eggshell membrane
Caiman siamensis	To be catalogued	Quaternary	No locality data given	Eggshell membrane
Alligator mississipiensis	To be catalogued	Quaternary	Jacksonville, FL, US	Eggshell membrane
Protoceratops andrewsi	IGM 100/1021	Cretaceous	Djadochta Fm., Mongolia	Eggshell
Maiasaura peeblesorum	YPM VP PU 023464	Cretaceous	Two Medicine Fm., Teton County, MT, US	Eggshell
Maiasaura peeblesorum	YPM PU 22523	Cretaceous	Two Medicine Fm., Teton County, MT, US	Eggshell
Mussaurus patagonicus	To be catalogued	Triassic	Laguna Colorada, Santa Cruz, Argentina	Eggshell
Saltasaurid	STIPB E360	Cretaceous	Sanagasta, La Rioja, Argentina	Eggshell
Titanosaurid	YPM PU 21158	Cretaceous	Lower Danien, Aix-en-Provence, France	Eggshell
Heyuannia huangi	NMNS CYN-2004-DINO-05	Cretaceous	Yuanpu Fm., Jiangxi, China	Eggshell
Microtroodontid	IGM 100/1323	Cretaceous	Djadochta Fm., Gobi, China	Eggshell
Microtroodontid	MAE 14-40	Cretaceous	Djadochta Fm., Gobi, China	Eggshell
Large Troodontid	YPM VP PU 023259	Cretaceous	Two Medicine Fm., Teton County, MT, US	Eggshell

Large Troodontid	PFMM-0014003517	Cretaceous	Chichengshan Fm., Zhejiang, China	Eggshell
Large Troodontid	AMNH FARB 6631	Cretaceous	Djadochta Fm., Gobi, China	Eggshell
Large Troodontid	IGM 100/1003	Cretaceous	Djadochta Fm., Gobi, China	Eggshell
Deinonychus antirrhopus	AMNH 3015	Cretaceous	Cloverly Fm., Big Horn County, MT, US	Eggshell
Enantiornithine	IGM 100/1339	Cretaceous	Djadochta Fm., Gobi, China	Eggshell
Psammornis rothschildi	ZFMK 23a:III/c/23	Quaternary	Djokran, Algeria	Eggshell
Rhea Americana	YPM ORN 24444	Quaternary	Bozeman, MT, US	Eggshell
Dromaius novaehollandiae	YPM ORN 24447	Quaternary	Bozeman, MT, US	Eggshell
Gallus domesticus	YPM ORN 23146	Quaternary	New Haven, CT, US	Eggshell membrane
Gallus domesticus	YPM ORN 23146	Quaternary	New Haven, CT, US	Eggshell

2. Method details

Histology

A sample of the white, egg-shaped halo surrounding one of the *Protoceratops* embryos in IGM 100/1021 was extracted, and subsequently embedded in epoxy resin. Since the crumbly, white halo was surface-exposed, epoxy resin was in direct contact and stabilized the halo against disintegration during the following cutting (diamond-blade saw) and polishing process (to a thickness of 30 µm). The black egg-shaped halo surrounding *Mussaurus* embryos in MPM-PV 1821 was sampled enclosed by limestone sediment, resin-embedded, cut and polished.

Histological sections cleaned with 70 % ethanol and photographed using a Leica MZ16 dissecting microscope with Optronics camera attachment. Leica Application Suite Core software was used for photography with a white balance presetting. The schematic drawing of the soft-shelled *Protoceratops* egg microstructure was based on the microphotographs shown in Fig. 2a, c and redrawn in Adobe Illustrator.

Extant eggshell membrane extraction

Extant *Caiman*, *Alligator*, *Emys*, *Mesoclemmys*, *Phrynops*, and *Gallus* eggshell (see Supplementary table 2 for sample data) were surface-cleaned with 70% ethanol, and incubated in 2M hydrochloric acid (aq) until structural disintegration was reached. In this way, the eggshell membranes detached from other eggshell organic residues. Shell membranes were collected, rinsed in deionized water, and air dried onto microscope glass slides. Samples were dehydrated to guarantee comparability with fossil eggshell samples. All eggshell membranes were subjected to the same Raman spectroscopic protocol as the *in situ* hard- and soft-shelled fossil and extant eggshells.

***In situ* Raman microspectroscopy and statistical analyses**

Raman microspectroscopy was performed immediately after surface-cleaning all investigated specimens (n=26 eggshell and n=9 sediment samples) with 70% ethanol, using a Horiba LabRam HR800 in the Department of Geology and Geophysics at Yale University with 532 nm excitation (20mW at the sample surface). The spectra were obtained in LabSpec 5 software (spectra acquisition, standard spike removal). The scattered Raman light was detected by an electron multiplying charge-coupled device (EM-CCD) after being dispersed with a 600

grooves/mm grating and passed through a 200 μm slit (hole size 300 μm). The spectrometer was calibrated using the first order Si band at 520.7 cm^{-1}. Ten spectra were accumulated in the 100–2000 cm^{-1} region for 20 s exposure time each. All spectra were analyzed in SpectraGryph 1.2 spectroscopic software (adaptive baseline, 50%, no offset, minimally smoothed through rectangular averaging over an interval of 4 points) and an automated peak search was performed (threshold 5.00%, prominence 3, Fig. 2b, d).

Eggshell (n=26), and sediment (n=9) wavenumber-spectral data were selected for their intensity and exact Raman shifts (outlined in Wiemann et al.[38], please find the data sets for the sediment-eggshell analysis, and the hard/soft eggshell analyses listed in the Supplementary Tables 1-2) (431cm^{-1} – 1806 cm^{-1}), and compiled in a data matrix (variance-covariance matrix). Two data set were generated (different peaks were extracted): First, a data set covering signals of organics in both eggshells and sediments were collected, and secondly, a data set covering protein (for extant samples) and PFP (for fossil samples) eggshells was compiled. The peaks used for each data set are listed in the Figs. 3a and b.

The first data set (Fig. 3a) was converted into a variance-covariance matrix, sediment and eggshell samples were identified, and a discriminant analysis was run in PAST 3.0 software. Convex hulls in the final analysis shown in Fig. 3a were drawn based on sample identity, and characterstic differences between sediment and eggshell organics are listed by Raman shift and band assignment.

The second data set (Fig. 3b) was also converted into a variance-covariance matrix, and biomineralized and non-biomineralized egg proteins (extant samples) and PFPs (fossil samples) were identified. Hard-shelled eggs were treated as biomineralized samples, while membranes and soft-shelled eggs (also egg membranes) were treated as non-biomineralized egg

proteins/PFPs. A discriminant analysis was run in PAST 3.0 software, and convex hulls in the final plot were drawn based on sample identity. Key differences between fossil and extant biomineralized (=hard-shelled), and non-biomineralized (=truly soft-shelled/membranes) egg proteins/PFPs are listed for each group. The key characteristics identified for biomineralized egg proteins/PFPs, namely chelating ligands, are present in extant biomineralized eggs, and preserve in fossil ones. Carbonyls, O-, and N-heterocycles act as proxies for biomineralization of eggshell proteins/PFPs.

Therefore, an additional cluster analysis run in PAST 3.0 software (UPGMA, Rho, one-way, unconstrained) was based on this sample set (shown in Fig. 4), and the resulting topology was redrawn in Mesquite software. Exploiting the biomineralization signal present in eggshell proteins and PFPs allows to compare fossil and extant eggshell materials (i.e., analysing whether eggshell were hard- or soft-shelled). Since all fossil eggshells suffer to a certain extent from diagenetic mineral precipitation, mineral composition of fossil eggshells is not informative for this purpose. Originally soft eggshell can be diagenetically calcified through phosphatization (i.e. Mongolian *Protoceratops* eggshell), or covered in clay minerals and diagenetic calcite.

We use untreated fossil, and untreated and decalcified extant (shell membranes) eggshell for analysing proteins (extant specimens) and protein fossilization products (fossil specimens). The eggshell protein phase organizes in hard-shelled eggs calcite crystal precipitation through abundant and characteristic chelating functional groups (shown in Fig. 3b). Based on the signal validation in Fig. 3b, a simple spectral cluster analysis focusing on protein and PFP can place the *Mussaurus* and *Protoceratops* eggshells in groups of either biomineralized or non-biomineralized samples. Since protein fossilization products retain both, a prominent phylogenetic and a tissue-type-specific signal, use of only untreated extant eggshells for the

cluster analysis would foster phylogenetic attraction of the fossil samples. However, since we aimed for the biomineralization signal in the protein/PFP phase, we also decalcified extant eggshells, and added them to the analysis as both, untreated and decalcified material. By doing this, we allow sample sorting based on the biomineralized signal rather than the phylogenetic signal. Thus, even soft-shelled dinosaur eggshell would not be phylogenetically attracted to, e.g., calcified bird eggshell (since modern birds lay exclusively hard-shelled eggs), but cluster based on the biomineralized signal in their protein/PFP phase with other soft eggs. Extant eggshells that do not produce the required protein signal during the used Raman point analysis, such as *Alligator*, *Caiman*, *Emys*, *Mesoclemmys*, and *Phrynops* eggs which exhibit a substantially higher crystallinity in their outer eggshell layers than dinosaur and bird eggs, could not be included among the hard-shelled samples (since there is not signal to analyse), but were added after decalcification in from of eggshell membranes to the soft-shelled samples.

Randomization cannot be applied to this study, because Raman spectra are characteristic for every sample, and can be taxonomically assigned at a glance based on their unique and distinctive taphonomic and compositional signatures. Also, we do not use any statistics that would require randomization. Samples were grouped together based on their identity (eggshell versus sediment), and their degree of biomineralisation (biomineralised versus non-biomineralised). The Principal Component Analysis and Discriminant Analysis shown in the Figs. 3, 4 suggests that samples group based on their organic phase as eggshell or sediment, and as biomineralised or non-biomineralised.

Spectral data were analysed 'blinded' for the hierarchical cluster analysis, and sample identity was only revealed in the result of the analysis. Otherwise, blinding did not apply for our

study, since Raman spectra of different eggshells contain characteristic spectral features, and are readily identifyable even without associated specimen information.

An Ancestral state reconstruction was performed (n=112 diapsid taxa). To reconstruct the ancestral nature of dinosaur eggshell, eggshells of both extant and fossil taxa have to be included. However, our assessment of original eggshell biomineralization is a novel approach, and this information is not available for eggshells other than the ones analyzed in this study. Therefore, our comprehensive Ancestral state reconstruction relies on the less accurate, 'traditional' coding based on eggshell mechanical properties, i.e. soft, semi-rigid, and rigid eggshell. These mechanical codings are tied to the fraction of the total eggshell thickness based on the shell membrane, and identified eggs as soft < 50% - 67% = semi-rigid < rigid. A mechanically soft eggshell includes (*sensu* Kusuda et al. 2013 and Packard et al. 1982) non-biomineralized eggs, such as *Protoceratops* and *Mussaurus*, as well as eggs with thin eggshell mineral patches, and a very thin eggshell mineral crust. Both, parsimony- and likelihood-based approaches were run in Mesquite 3.4 software[46]. In order to extrapolate eggshell mechanical properties (soft, semi-rigid and rigid) in extinct taxa showing both a membrane and a calcitic layer, such as in *Massospondylus*, we applied the definition used in extant taxa for the categorization of lizard and turtle eggs[6-7,47] (see Supplementary Information for more detailed methods).

3. Comparison of *Protoceratops*, *Mussaurus*, and soft turtle (*Chelydra*) eggshell

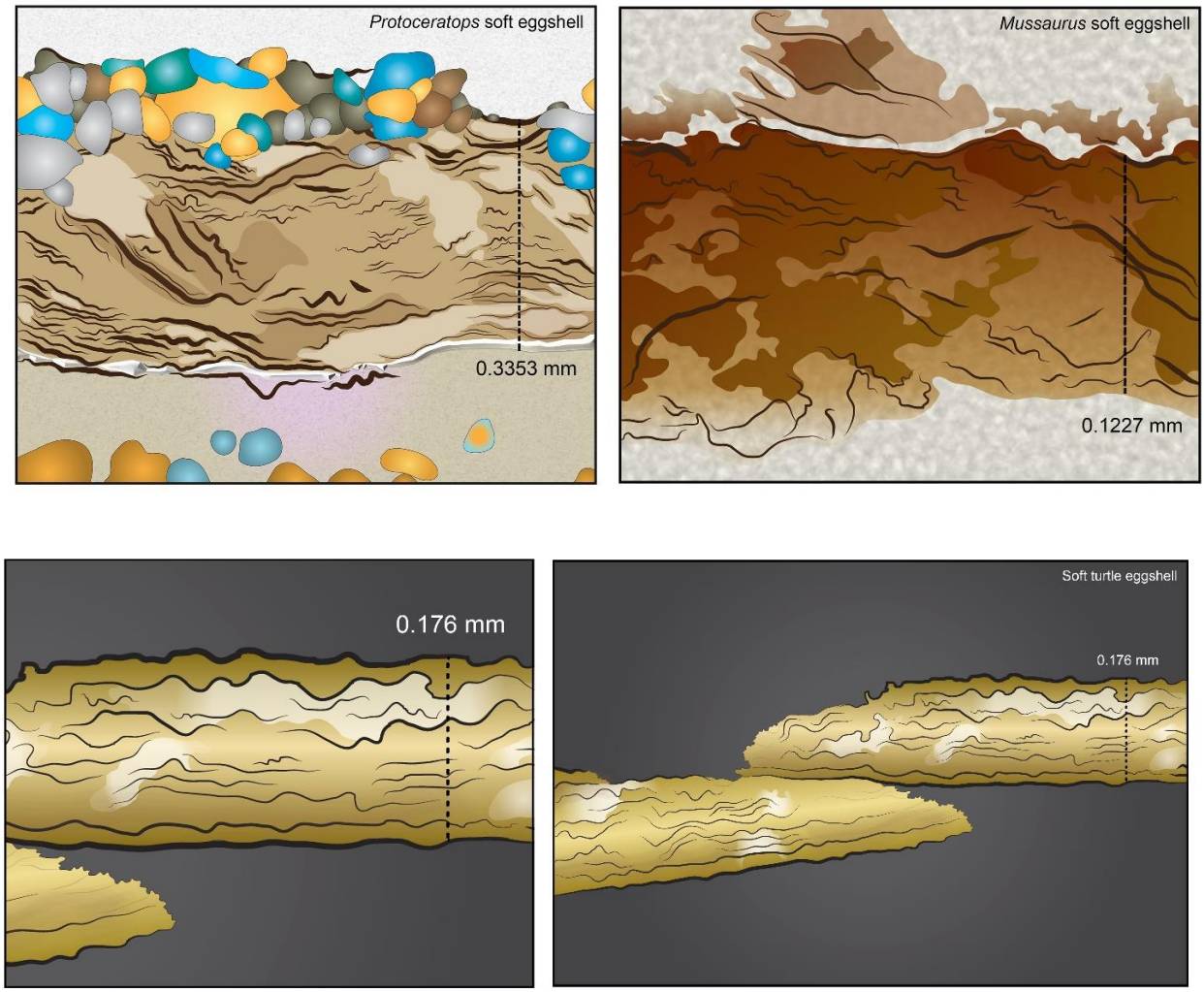

Supplementary Figure 1: Schematic drawing of soft dinosaur eggshells (top row: left is *Protoceratops* eggshell; right is *Mussaurus* eggshell) and soft turtle eggshells (*Chelydra* (YPM uncatalogued), drawing on the left is enlarged based on the drawing on the right).

4. Definitions and Raman mapping of *Mussaurus* eggshell

Organic phase: All biomolecules or their fossilization products contained in the eggshell and its associated shell membrane. This includes all proteins, polysaccharides, lipids, and incorporated metabolites.

Eggshell protein phase: All eggshell proteins involved in the formation of the eggshell organic matrix/spongy layer. This includes also eggshell membrane proteins.

Eggshell membrane: A protein-based structure directly below the eggshell. This is, contrary to the two terms listed above, a structural and not a compositional specification.

Under the given Raman spectroscopic setup (see Methods Summary), *Mussaurus* eggshell thin sections were mapped over the area photographed in Supplementary Figure 2 at 2 seconds exposure time, with 2 accumulations. The smooth surface texture allowed accurate compound mapping, and all maps were obtained over eggshell and sediment area of the thin section to test for compound contamination. Protein fossilization products, amide I signals indicative of peptide bonds, and C-S vibrations (thiols, S-heterocycles [=S-hcs], and thioethers) were mapped out based on their diagnostic Raman bands. The analyses shown in main text Figs. 2, 3, and 4 suggested endogeneity of these compounds to fossil eggshells. The Raman maps shown below corroborate this result: N- and S-heterocyclic compounds, as well as peptide bonds (or diagenetic amides) do not extend into the immediately adjacent sediment matrix. *Protoceratops* thin sections could not be subjected to Raman mapping due to the crumbly nature of eggshell and sediment.

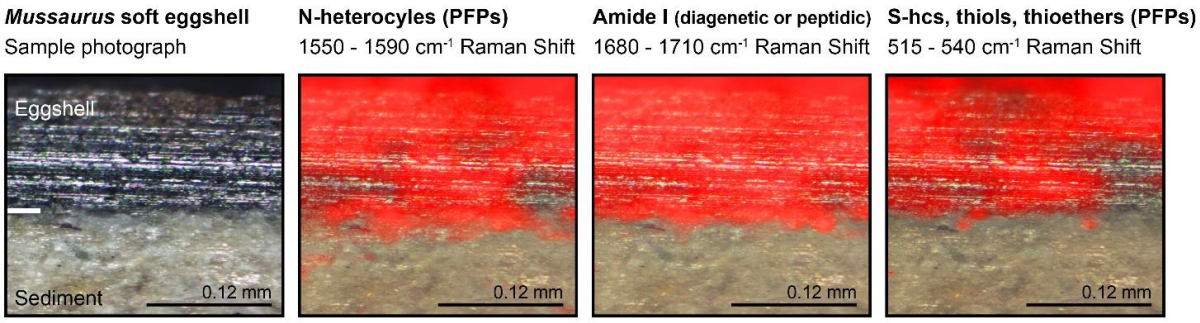

Supplementary Figure 2: Raman mapping of protein fossilization products and peptide bonds over the thin section (n=1) of *Mussaurus*. Three different Raman maps were obtained for 1 thin section. Each Raman map was acquired over the listed Raman ranges, at 2 s exposure time, and with 2 accumulations = 2 technical replicates. All three maps yielded independently similar results, and all results are shown.

Supplementary Tab. 2: Assignment of the peaks.

Raman shift	Band assignment	References
1650-1690	Peptide (Amide I), C=O stretch	Wiemann *et al*. (2018)
1550-1600	AGE/ALE, C=C stretch in (metal) imidazole ring	Wiemann *et al*. (2018)
1515-1520	AGE/ALE, N-H deformation	Wiemann *et al*. (2018)
1430-1440	Peptide, AGE/ALE, CH_3 antisymmetric deformation	Wiemann *et al*. (2018)
1400-1430	Peptide, AGE/ALE, C-N stretch	Wiemann *et al*. (2018)
1360-1370	Peptide, CH_3 symmetric deformation	Wiemann *et al*. (2018)
1340-1352	Peptide, AGE/ALE, (Metal) imidazole ring vibration	Wiemann *et al*. (2018)
1230-1250	Peptide (Amide III), C-C-N bending, C-N stretch, N-H bend	Wiemann *et al*. (2018)
1170-1180	Peptide, C-O-C stretch	Wiemann *et al*. (2018)
1080-1140	AGE/ALE, C-N stretch	Wiemann *et al*. (2018)
1050-1070	AGE/ALE, C-O stretch	Wiemann *et al*. (2018)

500	Peptide, Disulfide bridge	Wiemann *et al*. (2018)
520	Peptide, Disulfide bridge	Wiemann *et al*. (2018)
550	Peptide, Disulfide bridge	Wiemann *et al*. (2018)
650-680	Peptide/AGE/ALE, N-C=O bend	Wiemann *et al*. (2018)
750-790	Acid Extraction, C-Cl stretch	Wiemann *et al*. (2018)
830-840	Peptide/AGE/ALE, NH_2 stretch	Wiemann *et al*. (2018)
880	Peptide/AGE/ALE, CH_2 out-of-plane wagging	Wiemann *et al*. (2018)
908	Peptide/AGE/ALE, CH_2 out-of-plane wagging	Wiemann *et al*. (2018)
960	Peptide/AGE/ALE, CH out-of-plane deformation	Wiemann *et al*. (2018)
980	Peptide/AGE/ALE, CH_2=CH_2 out-of-plane deformation	Wiemann *et al*. (2018)
1700-1730	C=O stretch, C-C	Wiemann *et al*. (2018)
1780-1800	C=O stretch, C-C	Wiemann *et al*. (2018)
1956	C-C, C=C	Wiemann *et al*. (2018)

5. ACS: Extended material and methods

Ancestral character reconstruction was run to determine the ancestral condition of the eggshell at the divergence of Dinosauria. Two analyses were run: the first one considers Ornithodira, while the second includes all the major branches of Diapsida. The analysis including Diapsida is intended to determine if the condition at the base of Dinosauria reflects a derived state or the ancestral one in comparison to more basal amniote groups. 77 and 112 taxa representing respectively the clades Ornithodira and Diapsida were used to run the ancestral state reconstruction. The Supertrees were assembled to represent the phylogenetic relationships of the taxa included. We used the following phylogenies for editing the phylogenetic relationships of the taxa included: Simoes et al. (2018) for early amniotes and divergence of Sauropsida, Gauthier et al. (2012) for Lepidosauria, Ezcurra (2016) for Archosauromorpha, Field et al. (2014) and Bever et al. (2015) for the position of turtles, Nesbitt (2011) for Archosauria, Brochu (2003) for Crocodylia, Nesbitt et al. (2017) for Ornithodira, Langer et al. (2018) for Dinosauria, Butler et al. (2008), Apaldetti et al. (2018) for Sauropodomorpha, Carrano et al. (2012) and Brusatte et al. (2014) for Theropoda, and Prum et al. (2015) for Neornithes. One character, the mechanical properties of the eggshell, was coded as either soft, semi-rigid or rigid nature of the eggshell. These categories have clear, conventional definitions of purely mechanical, rather than chemical nature – we chose to run our Ancestral state reconstruction with mechanical eggshell codings contrary to chemical eggshell codings, simply to be able to include as many taxa as possible to gain a good phylogenetic coverage. Chemical coding of eggshells, i.e. characterizing shells as non-biomineralized versus biomineralized, would require the establishment of an entirely new data set, as this information is not readily available for any phylogenetically representative set of taxa. Since the key of our paper is to establish the mechanical nature of dinosaur eggshell, we based our ACS codings on the following mechanical categorizations: a mechanically soft eggshell shows a membrane that covers at least half of the overall thickness of the eggshell (this includes all originally non-biomineralized eggs, as well as eggs with a patchy or very thin mineral crust), a mechanically semirigid eggshell has a calcitic layer between half and two thirds of the overall thickness of the eggshell, and a mechanically hard eggshell has more than two/thirds of its overall thickness as calcitic (distinction is based on Kusuda et al. 2013; Packard et al. 1982). The categorization applied to the taxa included in the analyses is therefore following the current state of the art for squamates (Packard et al. 1982) and turtles (Kusuda et al. 2012). Ancestral state

reconstructions were then run under likelihood and parsimony in Mesquite (Maddison & Maddison 2018).

6. Character matrix

Number of characters: 1

Number of taxa: 112

Eggshell mechanical property: 0) soft eggshell; 1) semi-rigid; 2) rigid.

Sphenodon 1

Leiolepis belliana 0

Uromastyx aegyptius 0

Chameleo levigatus 0

Calotes emma 0

Agama agama 0

Phrynosoma platyrhinos 0

Morunasaurus annularis 0

Basiliscus basiliscus 0

Anolis carolinensis 0

Brachylophus fasciatus 0

Petrosaurus meanrsi 0

Delma borea 2

Coleonyx variegatus 2

Gonatodes albogularis 2

Lacerta viridis 0

Aspidoscelis tigris 0

Platysaurus imperator 0

Xantusia vigilis 0

Plestiodon fasciatus 0

Scincus scincus 0

Trachylepis quinquetaeniata 0

Pseudopus apodus 0

Elgaria multicarinata 0

Heloderma horridus 0

Varanus salvator 0

Anelytropsis papillosus 2

Amphisbaena fullginosa 0

Leptotyphlops dulcis 0

Xenopeltis unicolor 0

Casarea dussumieri 0

Morelia viridis0

Xenodermus javanicus 0

Lachesis muta 0

Pterodactyloid indet. china 0

Darwinopterus0

Beipiaopterus 0

Pterodaustro 2

Hamipterus tianshanensis 0

Kunpengopterus sp. 0

Alligator mississippiensis 2

Caiman yacare 2

Caiman siamensis 2

Crocodilus niloticus 2

Gharial 2

Herrerasaurus ?

Eoraptor ?

Telmatosaurus 2

Hypachrosaurus 2

Maiasaura 2

Heterodontosaurus ?

Thyreophora ?

Pachycephalosauridae ?

Protoceratops 0

Coronosauria + Leptoceratopsidae ?

Lesothosaurus ?

Saturnalia ?

Plateosaurus ?

Massospondylus 0

Lufengosaurus 0

Mussaurus 0

Diplodocoidea ?

Argentinian titanosaur 2

Saltasaurus 2

Romanian titanosaur 2

French titanosaur (Hypselosaurus) 2

Indian titanosaur 2

Spanish titanosaur 2

Coelophysis ?

Dilophosaurus ?

Ceratosaurus ?

Christodera 0

Torvosaurus 2

Megalosaurus ?

Spinosaurus ?

Lourinhasaurus 2

Tyrannosauroidea ?

Sinosauropteryx 2

Compsognathus ?

Scipionyx ?

Oviraptor sato et al 2

Citipati 2

Oviraptor 2

Gigantoraptor 2

Beibeilong sinensis 2

Heyuannia 2

Therizinosauroid china 2

Deinonychus 2

Dromaeosaur indet 2

Troodon formosus 2

Almas 2

Inga 2

Medium sized troodontid 2

large sized troodontid 2

Enanthiornithinae Romania 2

Enanthiornithinae Mongolia 2

Archaeopteryx ?

Confuciusornis ?

Argentinian enanthiornithinae 2

Ornithothoraces indet. Argentina 2

Ornithuromorpha indet. Argentina 2

Chinese troodontid 2

Dromaius novaehollandae 2

Apteryx 2

Struthio 2

Nothoprocta 2

Gallus domesticus 2

Anas 2

Tyto alba 2

Columba 2

Bonapartonykus 2

Gobibipus 2

Supplementary Tab. 3: References used for coding the condition in the taxa included in the analyses.

Taxa	**References**
Choristodera	Huo et al. (2009)
Lepidosauria	Mikhailov et al. (1996); Mikhailov & Michailov (1997); Packard et al. (1982); Packard & DeMarco (1992)
Crocodylia	Packard et al. (1982); Packard & DeMarco (1992); direct investigation in this study
Pterosauria	Ji et al. (2004); Lu et al. (2011); Chiappe et al. (2004); Wang et al. (2004); Junchang et al. (2005); Wang et al. (2014); Wang et al. (2017); Unwin & Deeming (2008)
Ornithischia	Horner (1982); Horner (1999); Grigorescu et al. (1994); Grigorescu (2010); direct investigation in this study

Sauropodomorpha	Reisz et al. (2013); Reisz et al. (2005); Sten et al. (2019); Zelenitsky & Modesto (2002); Chiappe et al. (1998); Jackson et al. (2008); Wilson et al. (2010); Sahni et al. (1994); Cousin et al. (1994); Hirsh et al. (1989); direct investigation in this study
Theropoda	Grillet-Tinner et al. (2006); Varricchio & Jackson (2016); Araujo et al. (2013); Mateus et al. (1998); Kundrat et al. (2008); Varricchio et al. (2002); Agnolin et al. (2012); Pei et al. (2017); Zelenitsky et al. (2002); Grillet-Tinner & Mackovicky (2006); Zelenitsky & Therrien (2008); Dyke et al. (2012); Fernandez et al. (2013); direct investigation in this study

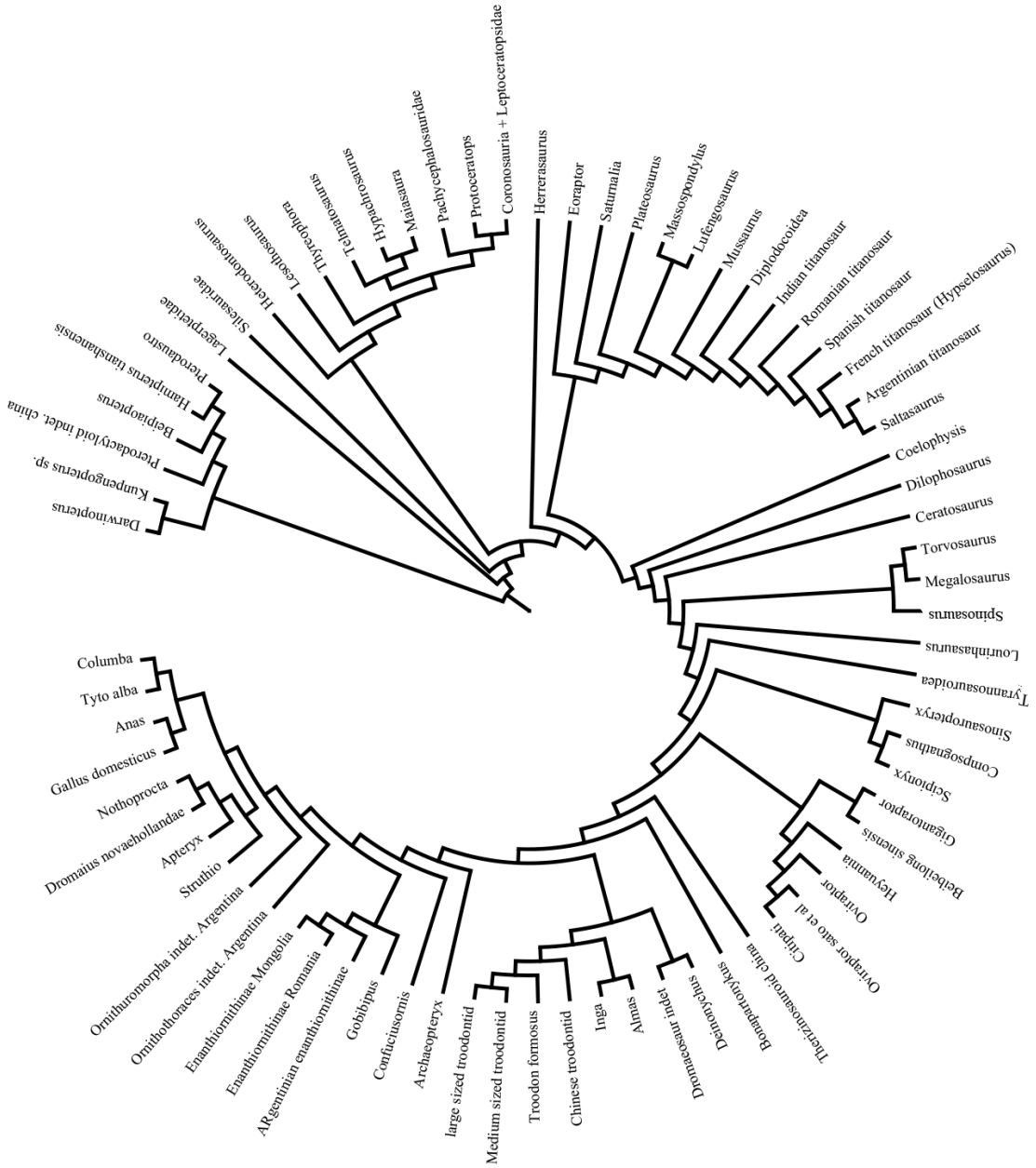

Supplementary Fig. 3: Supertree used for the character ancestral reconstruction analysis representing the phylogenetic relationships of Ornithodira.

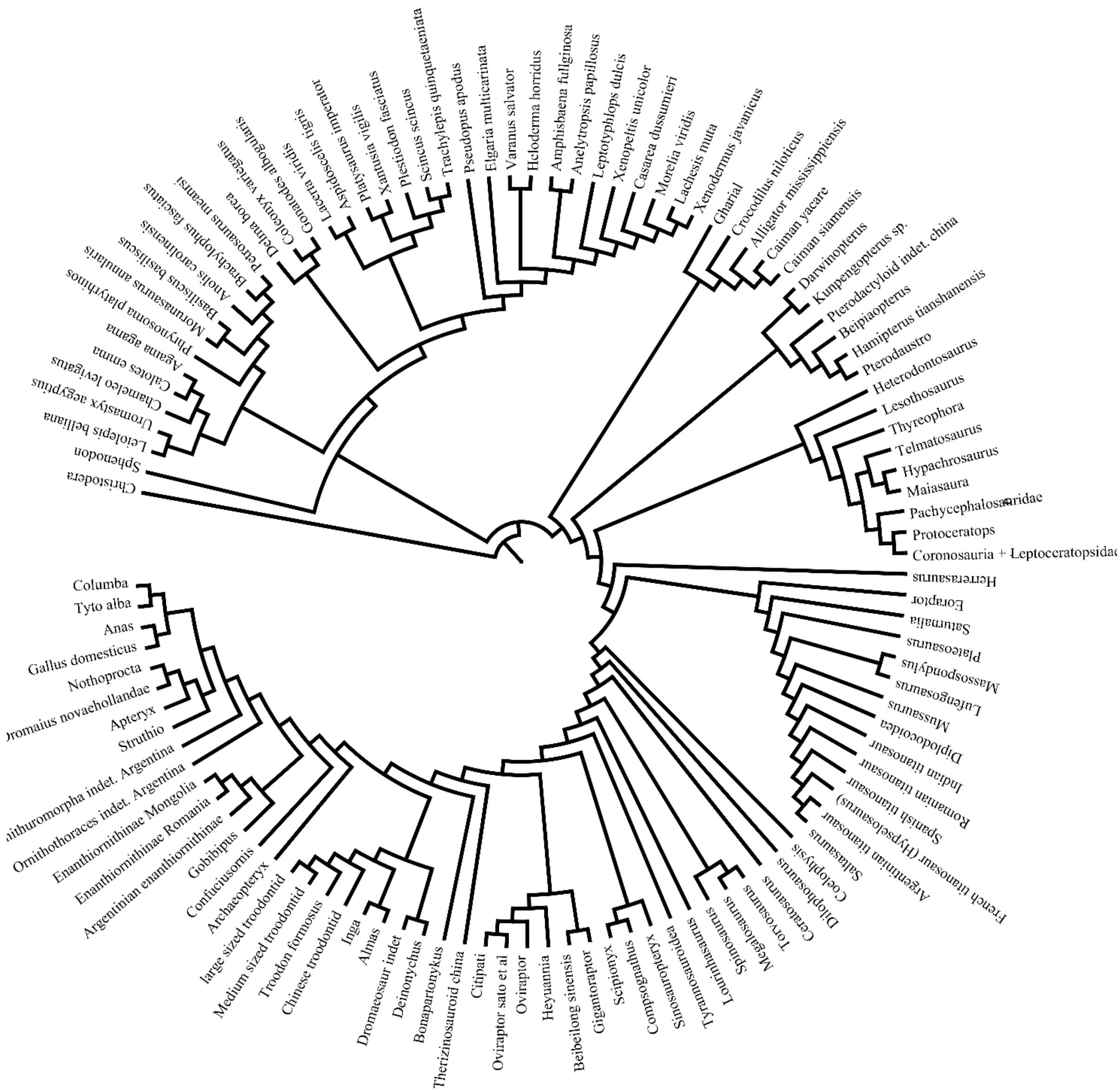

Supplementary Fig. 4: Supertree used for the character ancestral reconstruction analysis representing the phylogenetic relationships of the 112 amniote taxa included in this study.

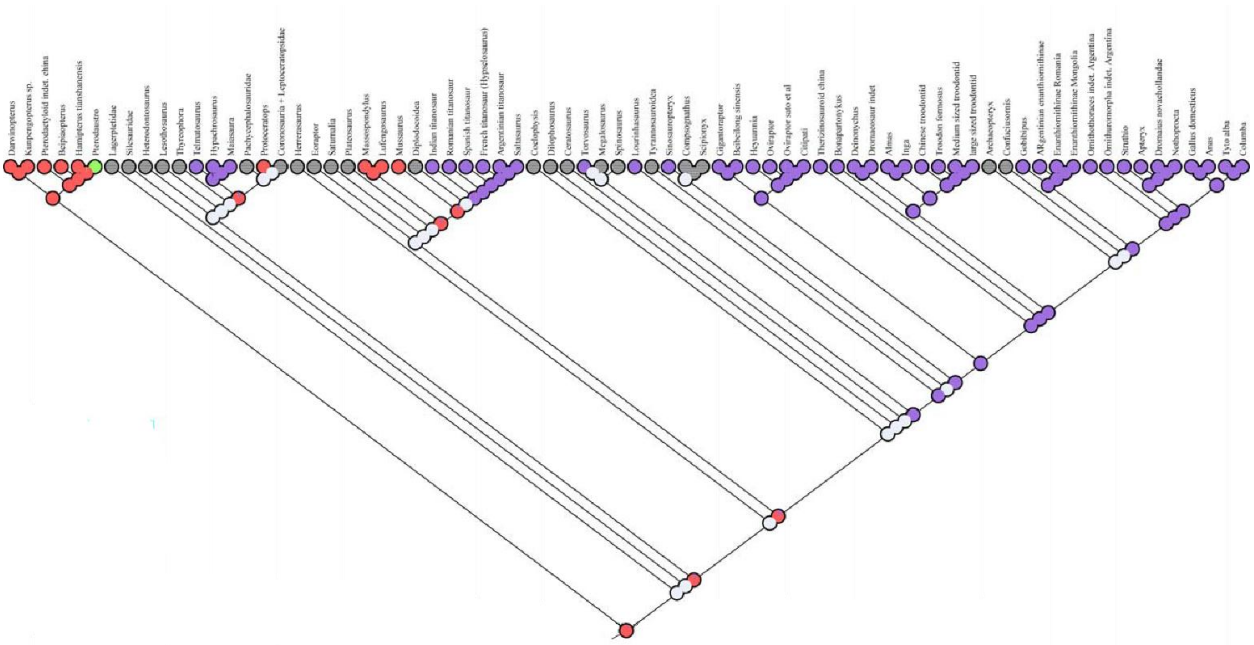

Supplementary Fig. 5: Likelihood based ancestral character reconstruction for character 1 in Ornithodira. Red indicates soft eggshell, green indicates semirigid and violet indicates rigid eggshell.

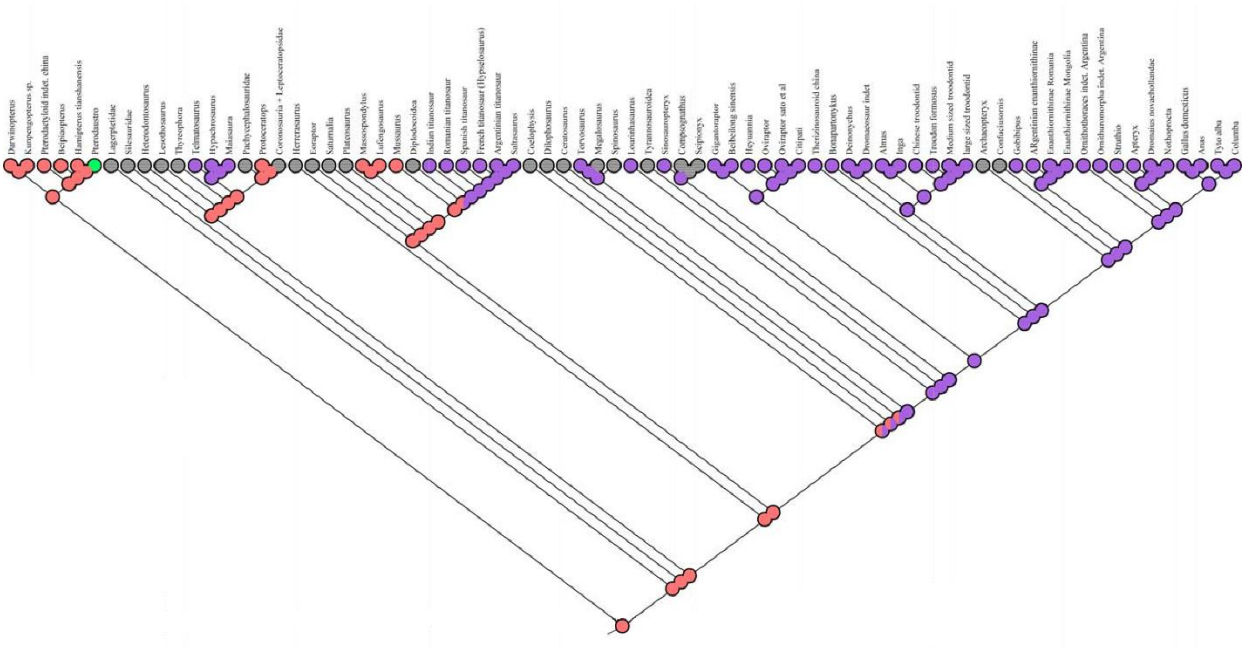

Supplementary Fig. 6: Parsimony based ancestral character reconstruction for character 1 in Ornithodira. Red indicates soft eggshell, green indicates semirigid and violet indicates rigid eggshell.

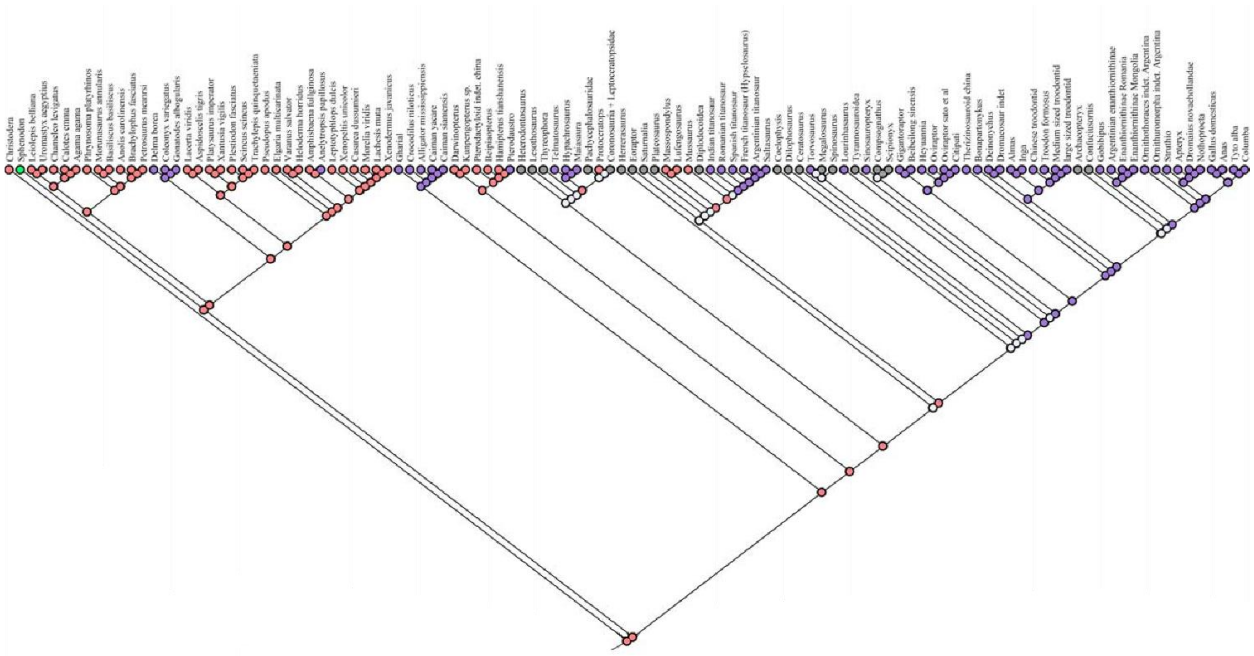

Supplementary Fig. 7: Likelihood based ancestral character reconstruction for character 1 in Diapsida. Red indicates soft eggshell, green indicates semirigid and violet indicates rigid eggshell.

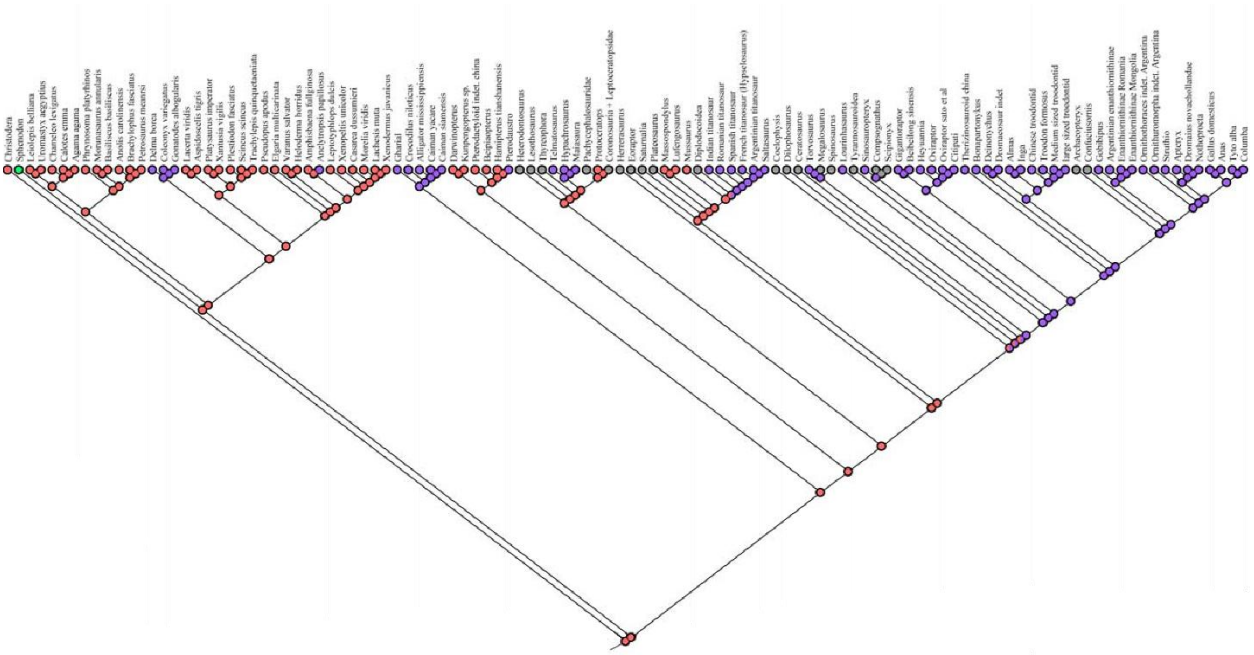

Supplementary Fig. 8: Parsimony based ancestral character reconstruction for character 1 in Diapsida. Red indicates soft eggshell, green indicates semirigid and violet indicates rigid eggshell.

Supplementary Tab. 4: Proportional likelihood values for states of character 1 in Ornithodira and Diapsida.

Ornithodira			
Node	Soft eggshell	Semi-rigid eggshell	Rigid eggshell
Ornithodira	0.96	0.001	0.038
Dinosauria	0.923	0.000	0.076
Saurischia	0.886	0.000	0.113
Diapsida			
Diapsida	0.989	0.0	0.006
Ornithodira	0.948	0.0	0.051
Dinosauria	0.908	0.0	0.091
Saurischia	0.867	0.0	0.132

7. Supplementary References

1. Simões, T. R., Caldwell, M. W., Tałanda, M., Bernardi, M., Palci, A., Vernygora, O., ... & Nydam, R. L. (2018). The origin of squamates revealed by a Middle Triassic lizard from the Italian Alps. *Nature*, *557*(7707), 706.

2. Luo, Z.-X. et al. New evidence for mammaliaform ear evolution and feeding adaptation in a Jurassic ecosystem. *Nature* **548**, 326–329 (2017)

3. Close, R. A., Friedman, M., Lloyd, G. T. & Benson, R. B. Evidence for a mid-Jurassic adaptive radiation in mammals. *Curr. Biol.* **25**, 2137–2142 (2015)

4. Gauthier, J. A., Kearney, M., Maisano, J. A., Rieppel, O., & Behlke, A. D. (2012). Assembling the squamate tree of life: perspectives from the phenotype and the fossil record. *Bulletin of the Peabody Museum of Natural History*, *53*(1), 3-308.

5. Ezcurra, M. D. (2016). The phylogenetic relationships of basal archosauromorphs, with an emphasis on the systematics of proterosuchian archosauriforms. *PeerJ*, *4*, e1778.

6. Bever, G. S., Lyson, T. R., Field, D. J., & Bhullar, B. A. S. (2015). Evolutionary origin of the turtle skull. *Nature*, *525*(7568), 239.

7. Field, D. J., Gauthier, J. A., King, B. L., Pisani, D., Lyson, T. R., & Peterson, K. J. (2014). Toward consilience in reptile phylogeny: miRNAs support an archosaur, not lepidosaur, affinity for turtles. *Evolution & development*, *16*(4), 189-196.

8. Nesbitt, S. J. (2011). The early evolution of archosaurs: relationships and the origin of major clades. *Bulletin of the American Museum of Natural History*, 1-292.

9. Brochu, C. A. (2003). Phylogenetic approaches toward crocodylian history. *Annual Review of Earth and Planetary Sciences*, *31*(1), 357-397.

10. Nesbitt, S. J., Butler, R. J., Ezcurra, M. D., Barrett, P. M., Stocker, M. R., Angielczyk, K. D., & Charig, A. J. (2017). The earliest bird-line archosaurs and the assembly of the dinosaur body plan. *Nature*, *544*(7651), 484.

11. Langer, M. C., Ezcurra, M. D., Rauhut, O. W., Benton, M. J., Knoll, F., McPhee, B. W., & Brusatte, S. L. (2017). Untangling the dinosaur family tree. *Nature*, *551*(7678), E1.

12. Butler, R. J., Upchurch, P., & Norman, D. B. (2008). The phylogeny of the ornithischian dinosaurs. *Journal of Systematic Palaeontology*, *6*(1), 1-40.

13. Apaldetti, C., Martínez, R. N., Cerda, I. A., Pol, D., & Alcober, O. (2018). An early trend towards gigantism in Triassic sauropodomorph dinosaurs. *Nature ecology & evolution*, *2*(8), 1227.

14. Carrano, M. T., Benson, R. B., & Sampson, S. D. (2012). The phylogeny of Tetanurae (Dinosauria: Theropoda). *Journal of Systematic Palaeontology*, *10*(2), 211-300.

15. Brusatte, S. L., Lloyd, G. T., Wang, S. C., & Norell, M. A. (2014). Gradual assembly of avian body plan culminated in rapid rates of evolution across the dinosaur-bird transition. *Current Biology*, *24*(20), 2386-2392.

16. Prum, R. O., Berv, J. S., Dornburg, A., Field, D. J., Townsend, J. P., Lemmon, E. M., & Lemmon, A. R. (2015). A comprehensive phylogeny of birds (Aves) using targeted next-generation DNA sequencing. *Nature*, *526*(7574), 569.

17. Kusuda, S., Yasukawa, Y., Shibata, H., Saito, T., Doi, O., Ohya, Y., & Yoshizaki, N. (2013). Diversity in the matrix structure of eggshells in the Testudines (Reptilia). *Zoological science*, *30*(5), 366-374.

18. Maddison, W. P. and D.R. Maddison. 2018. Mesquite: a modular system for evolutionary analysis. Version 3.51 http://www.mesquiteproject.org

19. Romer, A. S. (1957). Origin of the amniote egg. *The Scientific Monthly*, *85*(2), 57-63.

20. Sander, P. M. (2012). Reproduction in early amniotes. *Science*, *337*(6096), 806-808.

21. Hoffman, E. A., & Rowe, T. B. (2018). Jurassic stem-mammal perinates and the origin of mammalian reproduction and growth. *Nature*, *561*(7721), 104.

22. Hadek, R. (1965). The structure of the mammalian egg. *Int. Rev. Cytol*, *18*, 29-68.

23. Hou, L. H., Li, P. P., Ksepka, D. T., Gao, K. Q., & Norell, M. A. (2009). Implications of flexible-shelled eggs in a Cretaceous choristoderan reptile. *Proceedings of the Royal Society of London B: Biological Sciences*, rspb20092035.

24. Mikhailov, K. E., Bray, E. S., & Hirsch, K. F. (1996). Parataxonomy of fossil egg remains (Veterovata): principles and applications. *Journal of Vertebrate Paleontology*, *16*(4), 763-769.

25. Mikhailov, K. E., & Michailov, K. E. (1997). *Fossil and recent eggshell in amniotic vertebrates: fine structure, comparative morphology and classification* (pp. 1-80). Palaeontological Association.

26. Kusuda, S., Yasukawa, Y., Shibata, H., Saito, T., Doi, O., Ohya, Y., & Yoshizaki, N. (2013). Diversity in the matrix structure of eggshells in the Testudines (Reptilia). *Zoological science*, *30*(5), 366-374.

27. Zelenitsky, D. K., Therrien, F., Joyce, W. G., & Brinkman, D. B. (2008). First fossil gravid turtle provides insight into the evolution of reproductive traits in turtles. *Biology Letters*, *4*(6), 715-718.

28. Packard, M. J., Packard, G. C., & Boardman, T. J. (1982). Structure of eggshells and water relations of reptilian eggs. *Herpetologica*, 136-155.

29. Packard, M. J., & DeMarco, V. G. (1991). Eggshell structure and formation in eggs of oviparous reptiles. *Egg incubation: its effects on embryonic development in birds and reptiles*, 53-69.

30. Ji, Q., Ji, S. A., Cheng, Y. N., You, H. L., Lü, J. C., Liu, Y. Q., & Yuan, C. X. (2004). Palaeontology: pterosaur egg with a leathery shell. *Nature*, *432*(7017), 572.

31. Lü, J., Unwin, D. M., Deeming, D. C., Jin, X., Liu, Y., & Ji, Q. (2011). An egg-adult association, gender, and reproduction in pterosaurs. *Science*, *331*(6015), 321-324.

32. Chiappe, L. M., Codorniú, L., Grellet-Tinner, G., & Rivarola, D. (2004). Palaeobiology: Argentinian unhatched pterosaur fossil. *Nature*, *432*(7017), 571.

33. Wang, X., & Zhou, Z. (2004). Palaeontology: pterosaur embryo from the Early Cretaceous. *Nature*, *429*(6992), 621.

34. Junchang, L., & Qiang, J. (2005). A new ornithocheirid from the Early Cretaceous of Liaoning Province, China. *Acta Geologica Sinica-English Edition*, *79*(2), 157-163.

35. Wang, X., Kellner, A. W., Jiang, S., Wang, Q., Ma, Y., Paidoula, Y., & Li, N. (2014). Sexually dimorphic tridimensionally preserved pterosaurs and their eggs from China. *Current Biology*, *24*(12), 1323-1330.

36. Wang, X., Kellner, A. W., Jiang, S., Cheng, X., Wang, Q., Ma, Y., & Li, N. (2017). Egg accumulation with 3D embryos provides insight into the life history of a pterosaur. *Science*, *358*(6367), 1197-1201.

37. Unwin, D. M., & Deeming, D. C. (2008). Pterosaur eggshell structure and its implications for pterosaur reproductive biology. *Zitteliana*, 199-207.

38. Horner, J. R. (1982). Evidence of colonial nesting and ‘site fidelity’among ornithischian dinosaurs. *Nature*, *297*(5868), 675-676.

39. Schleich, H. H., & Kästle, W. (1988). *Reptile egg-shells*. G. Fischer.

40. Horner, J. R. (1999). Egg clutches and embryos of two hadrosaurian dinosaurs. *Journal of Vertebrate Paleontology*, *19*(4), 607-611.

41. Grigorescu, D., Weishampel, D. A. V. I. D., Norman, D. A. V. I. D., Seclamen, M., Rusu, M., Baltres, A., & Horner, J. R. (1994). Late Maastrichtian dinosaur eggs from the Hateg Basin (Romania). *Dinosaur eggs and babies*, 75-87.

42. Grigorescu, D. (2010). The “Tustea Puzzle”: hadrosaurid (Dinosauria, Ornithopoda) hatchlings associated with Megaloolithidae eggs in the Maastrichtian of the Hateg Basin (Romania). *Ameghiniana*, *47*(1), 89-97.

43. Reisz, R. R., Huang, T. D., Roberts, E. M., Peng, S., Sullivan, C., Stein, K., & Yang, C. (2013). Embryology of Early Jurassic dinosaur from China with evidence of preserved organic remains. *Nature*, *496*(7444), 210.

44. Reisz, R. R., Scott, D., Sues, H. D., Evans, D. C., & Raath, M. A. (2005). Embryos of an Early Jurassic prosauropod dinosaur and their evolutionary significance. *Science*, *309*(5735), 761-764.

45. Modesto, S. P., & Zelenitsky, D. K. (2002). Re-evaluation of the eggshell structure of eggs containing dinosaur embryos from the Lower Jurassic of South Africa. *South African Journal of Science*, *98*(7), 407-408.

46. Chiappe, L. M., Coria, R. A., Dingus, L., Jackson, F., Chinsamy, A., & Fox, M. (1998). Sauropod dinosaur embryos from the Late Cretaceous of Patagonia. *Nature*, *396*(6708), 258.

47. Jackson, F. D., Varricchio, D. J., Jackson, R. A., Vila, B., & Chiappe, L. M. (2008). Comparison of water vapor conductance in a titanosaur egg from the Upper Cretaceous of Argentina and a Megaloolithus siruguei egg from Spain. *Paleobiology*, *34*(2), 229-246.

48. Wilson, J. A., Mohabey, D. M., Peters, S. E., & Head, J. J. (2010). Predation upon hatchling dinosaurs by a new snake from the Late Cretaceous of India. *PLoS biology*, *8*(3), e1000322.

49. Sahni, A., & Khosla, A. (1994). Paleobiological, taphonomical and paleoenvironmental aspects of Indian Cretaceous sauropod nesting sites. *Gaia*, *10*, 215-223.

50. Cousin, R., Breton, G. E. R. A. R. D., Fournier, R. O. G. E. R., & Watté, J. P. (1994). Dinosaur egglaying and nesting in France. *Dinosaur eggs and babies*, 56-74.

51. Hirsch, K. F., Stadtman, K. L., Miller, W. E., & Madsen, J. H. (1989). Upper Jurassic dinosaur egg from Utah. *Science*, *243*(4899), 1711-1713.

52. Araújo, R., Castanhinha, R., Martins, R. M., Mateus, O., Hendrickx, C., Beckmann, F., & Alves, L. C. (2013). Filling the gaps of dinosaur eggshell phylogeny: Late Jurassic Theropod clutch with embryos from Portugal. *Scientific Reports*, *3*, 1924.

53. Grellet-Tinner, G., Chiappe, L. M., Norell, M. & Bottjer, D.Dinosaur eggs and nesting behaviors: a paleobiological investigation. *Palaeogeogr. Palaeoclimatol. Palaeoecol.* **232**, 294–321 (2006).

54. Mateus, I. *et al.* Upper Jurassic Theropod Dinosaur embryos from Lourinhã (Portugal) Upper Jurassic paleoenvironments in Portugal. *Mem. Acad. Ciênc. Lisb.* **37**, 101–109 (1998).

55. Kundrát, M., Cruickshank, A. R. I., Manning, T. W. & Nudds, J. Embryos of therizinosauroid theropods from the Upper Cretaceous of China: diagnosis and analysis of ossification patterns. *Acta Zool. (Stockh.)* **89**, 231–251 (2008).

56. Varricchio, D. J., Horner, J. R. & Jackson, F. D. Embryos and eggs for the cretaceous theropod dinosaur *Troodon formosus*. *J. Vertebr. Paleontol* **22**, 564–576 (2002).

57. Varricchio, D. J., & Jackson, F. D. (2016). Reproduction in Mesozoic birds and evolution of the modern avian reproductive mode. *The Auk*, *133*(4), 654-684.

58. Agnolin, F. L., Powell, J. E., Novas, F. E., & Kundrát, M. (2012). New alvarezsaurid (Dinosauria, Theropoda) from uppermost Cretaceous of north-western Patagonia with associated eggs. *Cretaceous Research, 35*, 33-56.

59. Pei, R., Norell, M. A., Barta, D. E., Bever, G. S., Pittman, M., & Xu, X. (2017). Osteology of a New Late Cretaceous Troodontid Specimen from Ukhaa Tolgod, Ömnögovi Aimag, Mongolia. *American Museum Novitates*, (3889), 1-47.

60. Zelenitsky, D. K., Modesto, S. P., & Currie, P. J. (2002). Bird-like characteristics of troodontid theropod eggshell. *Cretaceous Research*, *23*(3), 297-305.

61. Grellet-Tinner, G., & Makovicky, P. (2006). A possible egg of the dromaeosaur Deinonychus antirrhopus: phylogenetic and biological implications. *Canadian Journal of Earth Sciences*, *43*(6), 705-719.

62. Zelenitsky, D. K., & Therrien, F. (2008). Unique maniraptoran egg clutch from the Upper Cretaceous Two Medicine Formation of Montana reveals theropod nesting behaviour. *Palaeontology*, *51*(6), 1253-1259.

63. Zelenitsky, D. K., & Therrien, F. (2008). Unique maniraptoran egg clutch from the Upper Cretaceous Two Medicine Formation of Montana reveals theropod nesting behaviour. *Palaeontology*, *51*(6), 1253-1259.

64. Dyke, G., Vremir, M., Kaiser, G., & Naish, D. (2012). A drowned Mesozoic bird breeding colony from the Late Cretaceous of Transylvania. *Naturwissenschaften*, *99*(6), 435-442.

65. Schweitzer, M. H., Jackson, F. D., Chiappe, L. M., Schmitt, J. G., Calvo, J. O., & Rubilar, D. E. (2002). Late Cretaceous avian eggs with embryos from Argentina. *Journal of Vertebrate Paleontology*, *22*(1), 191-195.

66. Fernández, M. S., García, R. A., Fiorelli, L., Scolaro, A., Salvador, R. B., Cotaro, C. N., & Dyke, G. J. (2013). A large accumulation of avian eggs from the Late Cretaceous of Patagonia (Argentina) reveals a novel nesting strategy in Mesozoic birds. *PLoS One*, *8*(4), e61030.